BULLETIN OF THE POLISH ACADEMY OF SCIENCES
TECHNICAL SCIENCES, Vol. 71(4), 2023, Article number: e146408
DOI: 10.24425/bpasts.2023.146408

Influence of the specific load on stability and vibrations of the multimember column with internal cracks

Krzysztof SOKÓŁ[1]* **and Krzysztof KULIŃSKI**[2]

[1] Department of Mechanics and Machine Design Foundations, Czestochowa University of Technology, Częstochowa, Poland
[2] Department of Civil Engineering, Czestochowa University of Technology, Częstochowa, Poland

Abstract. Slender systems are mostly studied when Euler's load or follower load is considered. The use of those types of external loads results in well-known divergence or flutter shape of the characteristic curve. In this study, one takes into account the specific load which allows one to obtain an interesting divergence – pseudo flutter shape of characteristic curves on the external load–vibration frequency plane. The curves can change inclination angle as well as one can observe the change in vibration modes along them. The shape of those curves depends not only on the parameters of the slender system but also on loading heads that induce the specific load. In this study, one considers the slender multimember system in which cracks are present and weaken the host structure. The results of theoretical as well as numerical simulations are focused on the influence of the parameters of the loading heads on vibrations, stability, and loading capacity of the investigated system as well as on the possibility of partial reduction of unwanted crack effect.

Key words: crack; specific load; column; flutter; divergence; vibrations.

1. INTRODUCTION

Columns also known in the literature as slender systems can be subjected to different types of conservative and non-conservative external loads. In most studies, one uses Euler's load [1–4] due to fact of simplicity of mathematical description as well as easy experimental research (the line of action of load always stays on the undeformed axis of the studied system). The characteristic curve of a system subjected to Euler's load (divergence instability) on the external load–vibration frequency plane has a negative inclination and constant vibration mode. This type of load can be realized by easily accessible equipment in the form of for example hydraulic cylinders.

The non-conservative loads are also studied, which mostly use Beck's force [5], generating flutter instability. This load can be used with the follower factor [6–11]. The mentioned factor can be calculated as a relation between the angle of force line of action and loaded end deflection angle. It is also worth mentioning experimental studies on non-conservative loads. Those studies are very problematic due to the rapidness of the instability phenomenon as well as the used elements (jet engines) which can induce the non-conservative load.

An investigation into the stability of slender systems leads to the paper [12] where one can read about hybrid systems. In relation to the specific parameters, those systems show flutter or divergence instability type. It has been presented (on the external load–vibration frequency plane) that transition between types of instability can be achieved in relation to structural parameters such as translational springs [13,14], rotational springs [13,15], systems of dampers [16], concentrated mass [14,17] and simultaneous action of conservative and non-conservative load [18].

The external load used in this study is called a specific load and is realized by a set of two heads. Heads have circular outlines [19] but in the scientific literature, one can find heads with parabolic outlines [20] or created from linear elements [21]. This load was described in work written by Tomski [21] where he showed results of theoretical, numerical as well as experimental studies. Mathematical models proposed by Tomski allow one to obtain the specific load with the use of follower force directed towards the pole, generalized force directed towards the pole, and force directed towards the variable pole by means of an extended element of infinite stiffness. Discussed types of loads generate characteristic curves plotted in Fig. 1. The stability phenomenon is strongly associated with slender systems. In [22] authors focused on the definition of dynamic instability regions. In their studies, one used moderately thick beams and frames and created mathematical models on the basis of Timoshenko's theory, while analysis was carried out with the perturbation method, among others. The Timoshenko and Euler (applied in this study) theories are used in relation to the slenderness factor which is calculated as the cross-sectional area and total length of the beam element ratio.

Studies with the use of beam elements were extended to the ones given in [23], where authors introduced an additional protective layer, while the external load was applied in the form of Euler's one.

*e-mail: krzysztof.sokol@pcz.pl

Manuscript submitted 2022-12-16, revised 2023-05-26, initially accepted for publication 2023-06-14, published in August 2023.

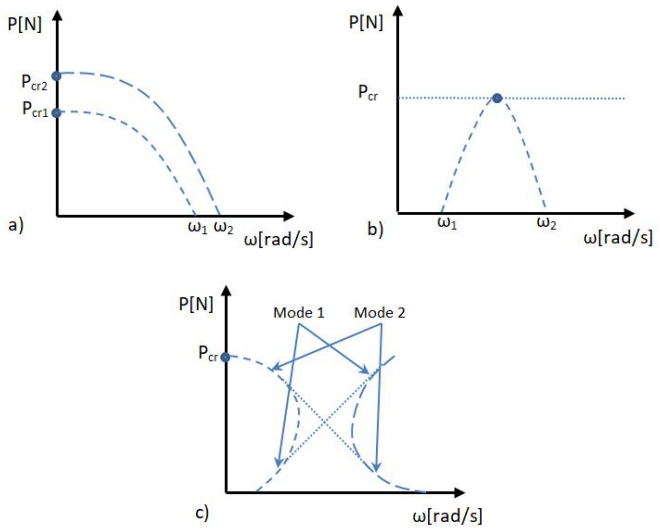

Fig. 1. Characteristic curves of slender system loaded by: a) Euler's load, b) Beck's load, c) specific load

The problems of analysis of the structures with cracks have been discussed by [24–29]. The authors presented the dynamic characteristics of the investigated systems as well as the results of studies on created mathematical models of cracks. According to the literature, one can find two ways of investigating cracks – as always open or as breathing ones. The effect of vibrations which will be combined with static deflection will affect the crack which is always open, completely closed, or open/closed. In the case when the static deflection will become greater than the amplitude of vibrations, the crack is always open type or it can (regularly) open and close – linear problem. While the static deflection is smaller than the amplitude of vibration, one can observe breathing cracks – it opens and closes as dependent on amplitude (non-linear case). Studies on breathing cracks were shown in [25, 30]. The studies on the subject literature can give the idea that in most papers cracks are treated as open. It can be also concluded that they are modeled in the form of cross-section area or as rotational springs with a pin (both massless). In the literature, one can also read about two different methods of studies on cracks. The first of them uses FEM analysis and requires the construction of a stiffness matrix [31] while the other one (used in this paper) presents strictly analytical problem formulation where one creates the matrix of coefficients on the basis of differential equations of motion supplemented by the boundary conditions. At this stage of work, one focuses only on linear aspects of the investigated problem while implementation of nonlinear elements will be done in future models.

In this study, the created mathematical model of a cracked element of a host structure is given as a massless rotational spring with a pin. The spring stiffness parameter takes into account the crack depth as well as the diameter of a cross-section. This paper presents the results of theoretical and numerical studies on the stability and vibrations of a slender system subjected to the specific load in which two cracks (always open) in the internal element are present. Investigations concern the influence of the size of the crack (spring stiffness) on vibration frequency, shape of characteristic curves, vibration modes, and bifurcation load magnitude as well as on the possibility of neglecting crack presence (reduction of bifurcation load) by the change in loading heads parameters.

2. BOUNDARY PROBLEM FORMULATION

Figure 2 shows an investigated slender system loaded by the specific load induced by a set of loading heads. The used circular shape of heads was proposed by Tomski [32, 33] and is not the only one available. The studied structure consists of continuous rod 1 (subscript 1). This rod will also be called an external member. Rods 2, 3, and 4 (subscripts 2, 3, 4) are created by the presence of cracks that divide an internal member. Cracks are marked as C_L (lower-located crack) and C_H (higher-located crack). The mentioned cracks are simulated by means of pins and rotational springs C_L and C_H, which gives the continuity of transversal displacements, longitudinal forces, bending moments, and deflection angles in the form of natural boundary conditions. The experimental verification of the mathematical model of a slender system with cracks modeled as a pin and rotational spring were presented in [34]. The proposed mathematical model despite some limitations like infinite stiffness of the support, lack of strain in the contact patch, linear springs, or taking into account only small deflections showed good accuracy with the experimental results and was upgraded for this study.

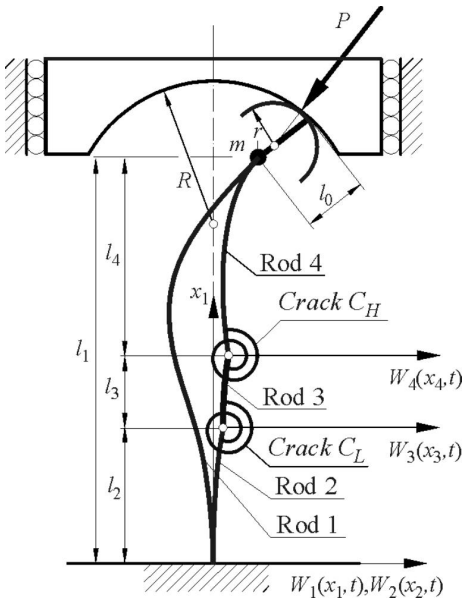

Fig. 2. Considered slender system – bent axes view

Length relation between rods can be written as $l_1 = l_2 + l_3 + l_4$. In the mathematical model also considers mass of the loading heads, shown in Fig. 2 as m. The external load proposed by Tomski [32] uses two loading heads. First one is called loading head and has radius $R$and is able to move only in the vertical direction. The radius of this head is calculated from the pole point placed on the undeformed axis of the column through

which passes the line of action of external force P. The second head is called load receiving one and has a radius r. The last parameter that must be explained is l_0 which stands for the distance between the end of the column and the head contact point. A similar mathematical model (because of its universality) was used in [35], where the study on control of the loading capacity by means of piezoceramic element was performed.

Notations and their units used in this paper are as follows: E_i – Young's modulus [GPa], J_i – a moment of inertia [m^4], A_i – cross-sectional area [m^2], ρ – material density [kg/m^3], P – external load [N], U_i, W_i – longitudinal and transversal displacements [m], R– loading head radius [m], r –load receiving head radius [m], m – mass [kg], l_0 – transom length [m], C_L, C_H – rotational spring stiffness [Nm].

The boundary problem is based on Hamilton's principle (1) according to which, in a given period, the motion of the system between the endpoint and the start point runs along a trajectory for which the function has a stationary value – minimum or inflection point depending on the distance between these points [36]:

$$\delta \int_{t_1}^{t_2} (T - V_1 - V_2)\,\mathrm{d}t = 0. \tag{1}$$

Energies (potential T and kinetic V) are given as:

$$T = \frac{1}{2}\sum_{i=1}^{4}\int_0^{l_i} \rho_i A_i \left[\frac{\partial W_i(x_i,t)}{\partial t}\right]^2 \mathrm{d}x_i + \frac{1}{2} m \left[\frac{\partial W_1(x_1,t)}{\partial t}\bigg|^{x_1=l_1}\right]^2, \tag{2}$$

$$\begin{aligned} V_1 =& \frac{1}{2}\sum_{i=1}^{4}\int_0^{l_i} E_i J_i \left[\frac{\partial^2 W_i(x_i,t)}{\partial x_i^2}\right]^2 \mathrm{d}x_i \\ &+ \frac{1}{2} C_L \left(\frac{\partial W_3(x_3,t)}{\partial x_3}\bigg|_{x_3=0} - \frac{\partial W_2(x_2,t)}{\partial x_2}\bigg|^{x_2=l_2}\right)^2 \\ &+ \frac{1}{2} C_H \left(\frac{\partial W_4(x_4,t)}{\partial x_4}\bigg|_{x_4=0} - \frac{\partial W_3(x_3,t)}{\partial x_3}\bigg|^{x_3=l_3}\right)^2 \\ &+ \frac{1}{2}\sum_{i=1}^{4} E_i A_i \int_0^{l_i} \left[\frac{\partial U_i(x_i,t)}{\partial x_i} + \frac{1}{2}\left(\frac{\partial W_i(x_i,t)}{\partial x_i}\right)^2\right]^2, \end{aligned} \tag{3}$$

$$\begin{aligned} V_2 =& P U_1(l_1,t) - \frac{1}{2} P l_0 \left(\frac{\partial W_1(x_1,t)}{\partial x_1}\bigg|^{x_1=l_1}\right)^2 \\ &+ \frac{1}{2} P r \left\{\left[\frac{\partial W_1(x_1,t)}{\partial x_1}\bigg|^{x_1=l_1}\right]^2 - \chi^2\right\} + \frac{1}{2} P \chi W^* \end{aligned} \tag{4}$$

In the above equations one uses the substitutions (5) and (6):

$$\chi = \frac{1}{R-r}\left(W_1(l_1,t) + (l_0 - r)\,\frac{\partial W_1(x_1,t)}{\partial x_1}\bigg|^{x_1=l_1}\right), \tag{5}$$

$$W^* = W_1(l_1,t) + \frac{\partial W_1(x_1,t)}{\partial x_1}\bigg|^{x_1=l_1}(l_0 - r) + r\chi. \tag{6}$$

On the basis of integration and variation operations, one can write (inter alia) equations of motion:

$$\begin{aligned} E_i J_i \frac{\partial^4 W_i(x_i,t)}{\partial x_i^4} + \rho_i A_i \frac{\partial^2 W_i(x_i,t)}{\partial t^2} - E_i A_i \frac{\partial}{\partial x_i}\left\{\left[\frac{\partial U_i(x_i,t)}{\partial x_i} \right.\right. \\ \left.\left. + \frac{1}{2}\left(\frac{\partial W_i(x_i,t)}{\partial x_i}\right)^2\right]\frac{\partial W_i(x_i,t)}{\partial x_i}\right\} = 0. \end{aligned} \tag{7}$$

The internal compressive longitudinal force has the form:

$$S_i(t) = -E_i A_i \left(\frac{\partial U_i(x_i,t)}{\partial x_i} + \frac{1}{2}\left[\frac{\partial W_i(x_i,t)}{\partial x_i}\right]^2\right). \tag{8}$$

A created mathematical model is described by the following set of geometrical and natural boundary conditions:

$$W_1(x_1,t)\big|_{x_1=0} = 0, \tag{9a}$$

$$\frac{\partial W_1(x_1,t)}{\partial x_1}\bigg|_{x_1=0} = 0, \tag{9b}$$

$$W_2(x_2,t)\big|_{x_2=0} = 0, \tag{9c}$$

$$\frac{\partial W_2(x_2,t)}{\partial x_2}\bigg|_{x_2=0} = 0, \tag{9d}$$

$$W_2(x_2,t)\big|^{x_2=l_2} = W_3(x_3,t)\big|_{x_3=0}, \tag{9e}$$

$$W_3(x_3,t)\big|^{x_3=l_3} = W_4(x_4,t)\big|_{x_4=0}, \tag{9f}$$

$$W_1(x_1,t)\big|^{x_1=l_1} = W_4(x_4,t)\big|^{x_4=l_4}, \tag{9g}$$

$$\frac{\partial W_1(x_1,t)}{\partial x_1}\bigg|^{x_1=l_1} = \frac{\partial W_4(x_4,t)}{\partial x_4}\bigg|^{x_4=l_4}, \tag{9h}$$

$$\begin{aligned} -E_3 J_3 \frac{\partial^2 W_3(x_3,t)}{\partial x_3^2}\Big|\Big|_{x_3=0} + C_L \left(\frac{\partial W_3(x_3,t)}{\partial x_3}\bigg|_{x_3=0}\right. \\ \left. - \frac{\partial W_2(x_2,t)}{\partial x_2}\bigg|^{x_2=l_2}\right) = 0, \end{aligned} \tag{9i}$$

$$\begin{aligned} E_2 J_2 \frac{\partial^2 W_2(x_2,t)}{\partial x_2^2}\bigg|^{x_2=l_2} - C_L \left(\frac{\partial W_3(x_3,t)}{\partial x_3}\bigg|_{x_3=0}\right. \\ \left. - \frac{\partial W_2(x_2,t)}{\partial x_2}\bigg|^{x_2=l_2}\right) = 0, \end{aligned} \tag{9j}$$

$$\begin{aligned} -E_4 J_4 \frac{\partial^2 W_4(x_4,t)}{\partial x_4^2}\bigg|_{x_4=0} + C_H \left(\frac{\partial W_4(x_4,t)}{\partial x_4}\bigg|_{x_4=0}\right. \\ \left. - \frac{\partial W_3(x_3,t)}{\partial x_3}\bigg|^{x_3=l_3}\right) = 0, \end{aligned} \tag{9k}$$

$$E_3J_3\frac{\partial^2 W_3(x_3,t)}{\partial x_3^2}\bigg|^{x_3=l_3} - C_H\left(\frac{\partial W_4(x_4,t)}{\partial x_4}\bigg|_{x_4=0} - \frac{\partial W_3(x_3,t)}{\partial x_3}\bigg|^{x_3=l_3}\right) = 0, \tag{9l}$$

$$E_2J_2\frac{\partial^3 W_2(x_2,t)}{\partial x_2^3}\bigg|^{x_2=l_2} + S_2\frac{\partial W_2(x_2,t)}{\partial x_2}\bigg|^{x_2=l_2} - E_3J_3\frac{\partial^3 W_3(x_3,t)}{\partial x_3^3}\bigg|_{x_3=0} - S_3\frac{\partial W_3(x_3,t)}{\partial x_3}\bigg|_{x_3=0} = 0, \tag{9m}$$

$$E_3J_3\frac{\partial^3 W_3(x_3,t)}{\partial x_3^3}\bigg|^{x_3=l_3} + S_3\frac{\partial W_3(x_3,t)}{\partial x_3}\bigg|^{x_3=l_3} - E_4J_4\frac{\partial^3 W_4(x_4,t)}{\partial x_4^3}\bigg|_{x_4=0} - S_4\frac{\partial W_4(x_4,t)}{\partial x_4}\bigg|_{x_4=0} = 0, \tag{9n}$$

$$E_1J_1\frac{\partial^2 W_1(x_1,t)}{\partial x_1^2}\bigg|^{x_1=l_1} + E_4J_4\frac{\partial^2 W_4(x_4,t)}{\partial x_4^2}\bigg|^{x_4=l_4} + P\frac{r-l_0}{R-r}\left(\frac{\partial W_1(x_1,t)}{\partial x_1}\bigg|^{x_1=l_1}(R-l_0) - W_1(x_1,t)\big|^{x_1=l_1}\right) = 0, \tag{9o}$$

$$E_1J_1\frac{\partial^3 W_1(x_1,t)}{\partial x_1^3}\bigg|^{x_1=l_1} + E_4J_4\frac{\partial^3 W_4(x_4,t)}{\partial x_4^3}\bigg|^{x_4=l_4} + P\frac{1}{R-r}\left(\frac{\partial W_1(x_1,t)}{\partial x_1}\bigg|^{x_1=l_1}(R-l_0) - W_1(x_1,t)\big|^{x_1=l_1}\right) - m\frac{\partial^2 W_1(x_1,t)}{\partial t^2}\bigg|^{x_1=l_1} = 0. \tag{9p}$$

$$S_1 + S_2 = P, \tag{10a}$$

$$S_2 = S_3 = S_4, \tag{10b}$$

$$U_1(x_1,t)\big|_{x_1=0} = 0, \tag{11a}$$

$$U_2(x_2,t)\big|_{x_2=0} = 0, \tag{11b}$$

$$U_1(x_1,t)\big|^{x_1=l_1} = U_4(x_4,t)\big|^{x_4=l_4}, \tag{11c}$$

$$U_2(x_2,t)\big|^{x_2=l_2} = U_3(x_3,t)\big|_{x_3=0}, \tag{11d}$$

$$U_3(x_3,t)\big|^{x_3=l_3} = U_4(x_4,t)\big|_{x_4=0}. \tag{11e}$$

The solution to the studied problem is carried out with the small parameter method [33–38] classified as a perturbative one. Those methods are used to determine approximate solutions for which there is no exact one.

3. RESULTS

The results of all numerical simulations are given in the form of non-dimensional parameters, where:

$$p = \frac{Pl_1^2}{E_1J_1+E_2J_2}, \tag{12a}$$

$$c_{\mathrm{L}} = \frac{C_Ll_1}{E_1J_1+E_2J_2}, \tag{12b}$$

$$c_{\mathrm{H}} = \frac{C_Hl_1}{E_1J_1+E_2J_2}, \tag{12c}$$

$$r_{21} = \frac{E_2J_2}{E_1J_1}, \tag{12d}$$

$$r_{32} = \frac{E_3J_3}{E_2J_2}, \tag{12e}$$

$$r_{43} = \frac{E_4J_4}{E_3J_3}, \tag{12f}$$

$$\zeta_{\mathrm{A}} = \frac{R}{l_1}, \tag{12g}$$

$$\zeta_{\mathrm{B}} = \frac{r}{R}, \tag{12h}$$

$$\zeta_{\mathrm{C}} = \frac{l_0}{R}, \tag{12i}$$

$$\zeta_{\mathrm{D}} = \frac{m}{(\rho_1A_1+\rho_2A_2)l_1}, \tag{12j}$$

$$d_2 = \frac{l_2}{l_1}, \tag{12k}$$

$$d_3 = \frac{l_3}{l_1}, \tag{12l}$$

$$\omega = \sqrt{\Omega^2\frac{(\rho_1A_1+\rho_2A_2)\,l_1^4}{E_1J_1+E_2J_2}}. \tag{12m}$$

Analysis of cracks in the studies systems was divided into two stages. In the first stage, the curves illustrating the change in the magnitude of the bifurcation load were plotted. The second part focuses on the change in the shape of characteristic curves and the presentation of vibration modes. All results presented in this paper are plotted at $r_{21} = r_{32} = r_{43} = 1$, $d_2 = 0.25$, $d_3 = 0.5$.

In the case when the lower crack-spring c_L is considered (Fig. 3) it can be observed that with an increase in ζ_A, the value of the bifurcation load decreases. In the whole presented range, the reduction of c_L stiffness has a small influence on the loading capacity.

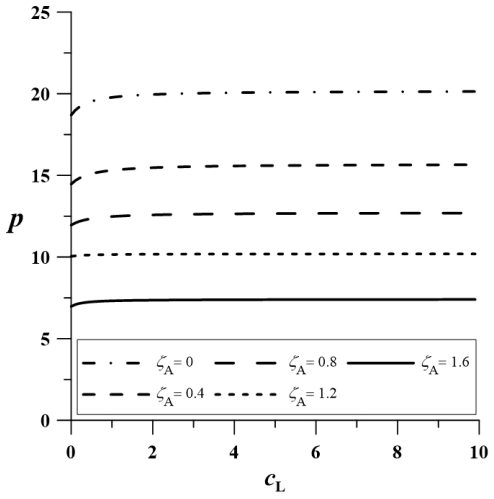

Fig. 3. Influence of c_L on bifurcation load magnitude at different ζ_A ($\zeta_B = 0.2$, $\zeta_C = 0.5$, $c_H = 10^6$)

This decrease is significantly smaller when compared to the results given in Fig. 4, which considers higher crack–spring with c_H stiffness. A decrease in c_H stiffness results in a more rapid decrease in loading capacity as well as one can observe that the magnitude of c_H has a greater influence on studied pa-

rameters than c_L. In this case, one concludes that an increase in the radius of the loading head ζ_A decreases the maximum external load magnitude, which is analogous to Fig. 3.

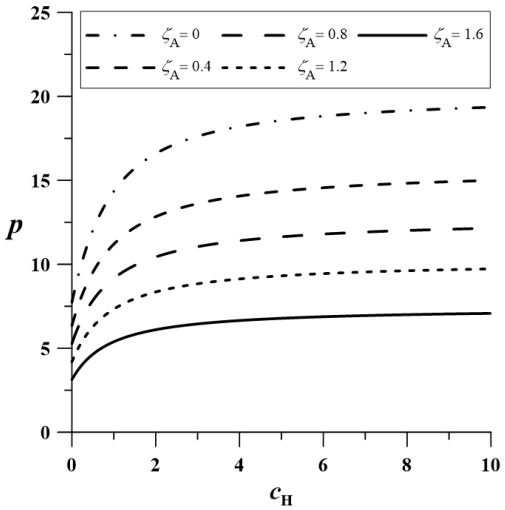

Fig. 4. Influence of c_H on bifurcation load magnitude at different ζ_A ($\zeta_B = 0.2$, $\zeta_C = 0.5$, $c_L = 10^6$)

Results of simulations on the influence of change in rotational spring stiffness on loading capacity at different ζ_B are given in Figs. 5 and 6. In the studied range of ζ_B, the reduction of maximum p magnitude can be observed at very weak c_L. When c_H is taken into account, the decrease in maximum external load magnitude is much greater and rapid. It can be stated that the greater ζ_B, the earlier reduction of loading capacity in relation to spring stiffness.

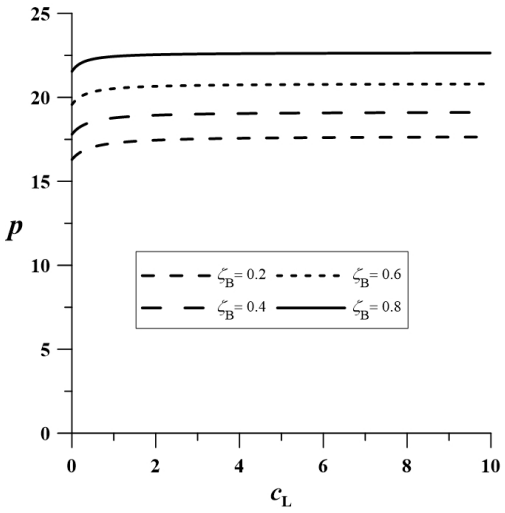

Fig. 5. Influence of c_L stiffness on bifurcation load magnitude at different ζ_B ($\zeta_A = 0.2$, $\zeta_C = 0.5$, $c_H = 10^6$)

The change in loading capacity under the influence of the reduction of spring stiffness at different transom lengths ζ_C is plotted in Figs. 7 and 8. It was stated that regardless of the magnitude of c_L and c_H, it is better to use a shorter transom (smaller

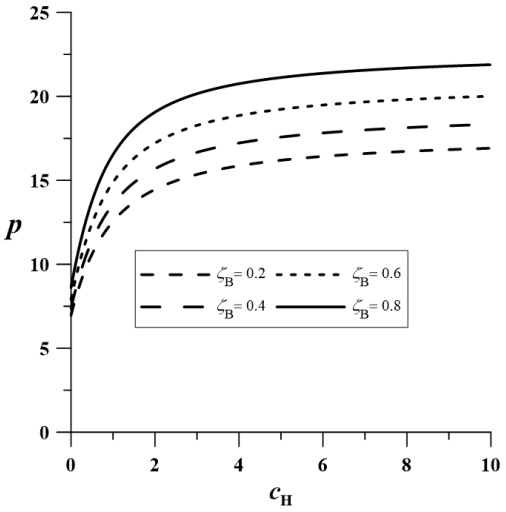

Fig. 6. Influence of c_H stiffness on bifurcation load magnitude at different ζ_B ($\zeta_A = 0.2$, $\zeta_C = 0.5$, $c_H = 10^6$)

magnitude of ζ_C), which results in a greater magnitude of bifurcation load. Moreover, analogous to the previously presented cases the reduction in lower spring stiffness has a much smaller influence on loading capacity than the reduction in stiffness of upper one.

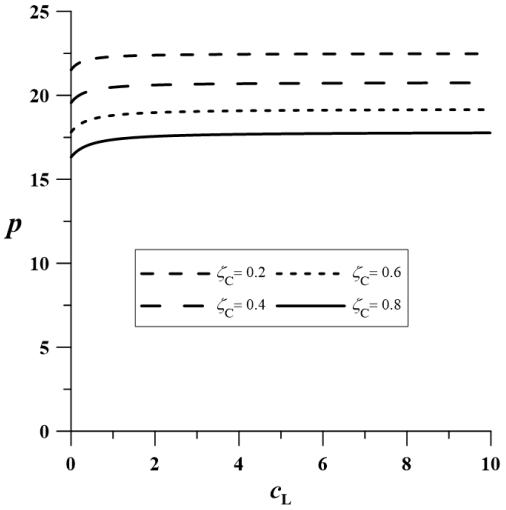

Fig. 7. Influence of c_L stiffness on bifurcation load magnitude at different ζ_C ($\zeta_A = 0.2$, $\zeta_B = 0.5$, $c_H = 10^6$)

The results allow one to state that one can find the change in parameters of the loading head, which gives a possibility of neglecting the crack presence of both lower and higher ones. An influence of loading head parameters is getting smaller along with an increase in the crack sizes (lower spring stiffness).

An influence of the magnitude of lower rotational spring stiffness c_L on vibration frequency as well as the shape of characteristic curves is presented in Figs. 9–11. A small change in vibration frequency magnitude was observed in all studied cases. All considered characteristic curves pass close to each

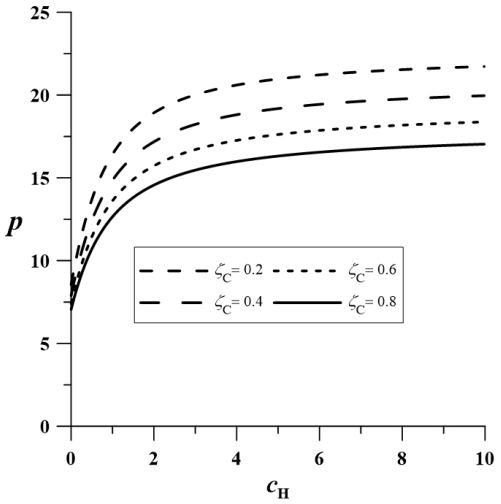

Fig. 8. Influence of c_H stiffness on bifurcation load magnitude at different ζ_C ($\zeta_A = 0.2$, $\zeta_B = 0.5$, $c_H = 10^6$)

other in their initial run (at a small magnitude of p); later the space between them increases. Moreover, the difference between curves at $c_L = 10$ and $c_L = 5$ is hardly visible. This confirms previous results in which the reduction of stiffness of c_L has a small influence on bifurcation load magnitude.

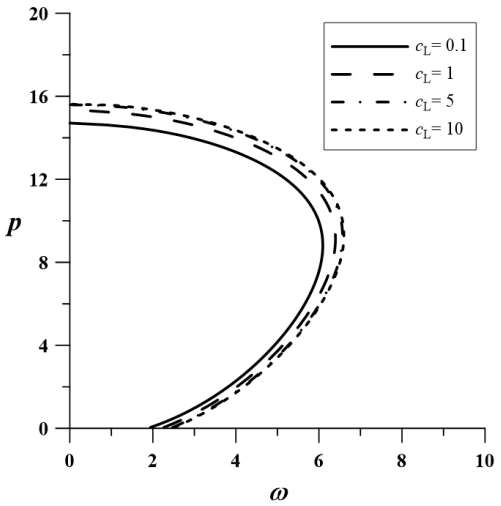

Fig. 9. Characteristic curves at different stiffness of c_L ($\zeta_A = 0.4$, $\zeta_B = 0.2$, $\zeta_C = 0.5$, $\zeta_D = 0.2$, $c_H = 10^6$)

The results of studies on the influence of weakening in connection of rods 3 and 4 (stiffness of spring c_H) are plotted in Figs. 12–14. In relation to Figs. 8–10, it can be easily observed that the change in c_H stiffness results in much greater differences in the shapes of characteristic curves. In the discussed cases, the reduction of c_H from $c_H = 10$ down to $c_H = 5$ reveals different runs above maximum vibration frequency magnitude (in relation to $c_L = 10$ and $c_L = 5$). Further stiffness reduction results in a more rapid reduction in bifurcation load magnitude. It should be stated that regardless of c_H stiffness all characteristic curves overlap or run very close to each other on the $p - \omega$ plane at low magnitude of external load.

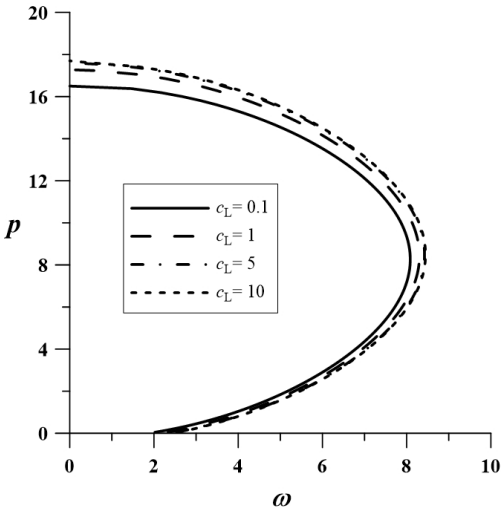

Fig. 10. Characteristic curves at different stiffness of c_L ($\zeta_A = 0.2$, $\zeta_B = 0.2$, $\zeta_C = 0.5$, $\zeta_D = 0.2$, $c_H = 10^6$)

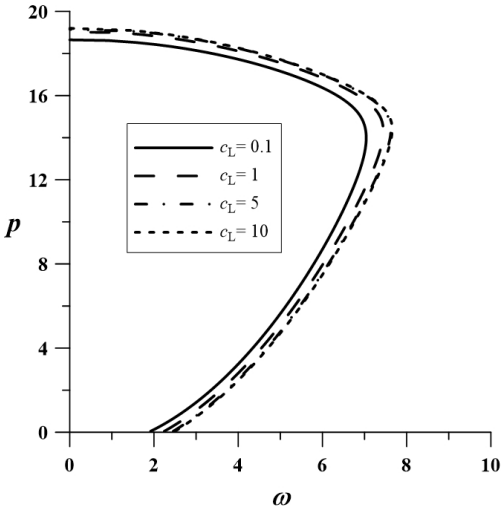

Fig. 11. Characteristic curves at different stiffness of c_L ($\zeta_A = 0.4$, $\zeta_B = 0.2$, $\zeta_C = 0.2$, $\zeta_D = 0.2$, $c_H = 10^6$)

Studies on characteristic curves were supplemented by the ones devoted to vibration modes. In calculations of vibration modes, the normalization condition of transversal displacements was applied in the form $w_1(0.5) = 0.1$.

The dashed line corresponds to rod 1 while the continuous represents the internal member composed of rods 2, 3, and 4. Due to the fact of studies on slender systems subjected to the specific load the vibration mode studies require checking vibration modes on positive and negative inclinations of the characteristic curve. As it was presented by Tomski [32] divergence – pseudo flutter systems change vibration modes along the characteristic curve from first (at positive inclination) to second (at negative inclination).

In Table 1 one has placed vibration modes computed at different magnitudes of rotational springs 0.1 and 5 and at different inclinations of characteristic curves. It can be concluded that at $c_L = 0.1$ in the first vibration mode, one can see much greater

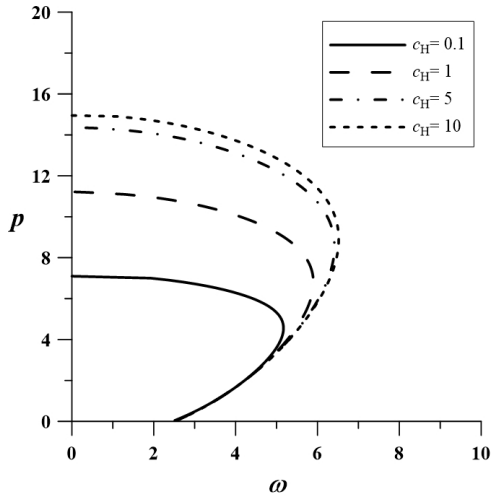

Fig. 12. Characteristic curves at different stiffness of c_H ($\zeta_A = 0.4$, $\zeta_B = 0.2$, $\zeta_C = 0.5$, $\zeta_D = 0.2$, $c_L = 10^6$)

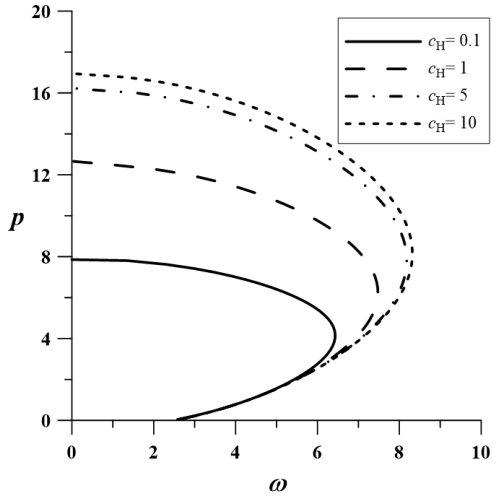

Fig. 13. Characteristic curves at different stiffness of c_H ($\zeta_A = 0.2$, $\zeta_B = 0.2$, $\zeta_C = 0.5$, $\zeta_D = 0.2$, $c_L = 10^6$)

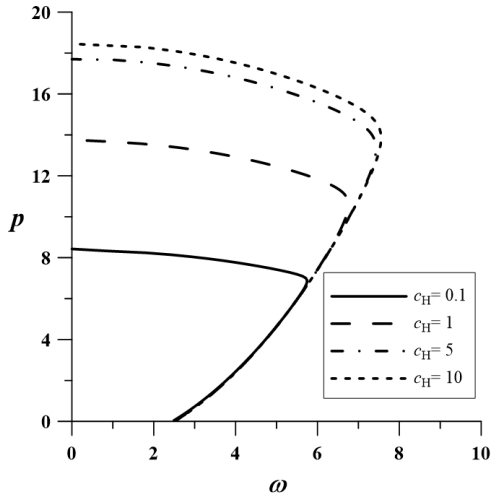

Fig. 14. Characteristic curves at different stiffness of c_H ($\zeta_A = 0.4$, $\zeta_B = 0.2$, $\zeta_C = 0.2$, $\zeta_D = 0.2$, $c_L = 10^6$)

differences in bent axes of rods than at $c_H = 0.1$ which determines the greater shift of the characteristic curves (at positive inclination) relative to the weaker upper end. The second mode of vibrations in the case of small c_H (greater crack) shows much greater differences than the corresponding mode at $c_L = 0.1$. As a result, the maximum load is lower at smaller c_H.

Table 1

Influence of the rotational springs stiffness (crack size) on vibration modes ($\zeta_A = 0.4$, $\zeta_B = 0.2$, $\zeta_C = 0.2$, $\zeta_D = 0.2$)

$c_L = 0.1$, $c_H = 5$	
$p = 2$	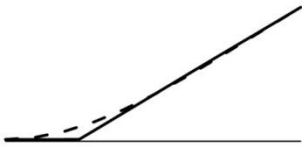
$p = 18$	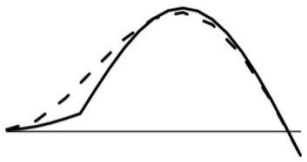
$c_L = 5$, $c_H = 0.1$	
$p = 2$	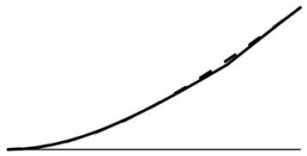
$p = 12$	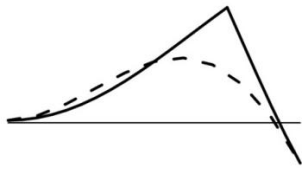

4. CONCLUSIONS

The main purpose of this study was to present the influence of the parameters of the loading heads on the control of stability and vibrations of a cracked column. Cracks were simulated with rotational springs. Implemented load generates divergence – pseudo flutter type of characteristic curve with initial positive inclination up to maximum vibration magnitude after which inclination changes to negative up to the instability point. Detailed conclusions are given in Section 3. In general, it can be stated that:

- The negative presence of cracks (like a reduction of the loading capacity) can be neglected by the change in the parameters of the loading heads. This can only be applied at smaller crack sizes (especially while the higher crack is considered). Shown results have confirmed that the use of the specific load gives a possibility of stability and vibration control by the change in the parameters of the loading structures.

- An increase of crack (reduction of spring stiffness) reduces loading capacity and changes the vibration frequency and modifies the shapes of characteristic curves.
- Characteristic curves under the change in crack size are being shifted on the external load–vibration frequency plane along with a change in their inclination angles.
- Cracks size affects vibration modes, which can be easily observed at their low stiffness.
- A much greater influence on loading capacity has the size of the higher crack than the lower one.

The applied research method and the mathematical model presented in this paper may constitute the basis for further scientific research where one should also consider the length of rod 3 (distance between cracks), length of rods 2 and 4 (location of crack from the support or the loaded end) or bending rigidity relationships. Having in mind that the change in parameters of the loading heads may reduce crack presence one can expect interesting studies on this subject.

The mathematical model used in this paper has some simplifications. One of them is lack of the internal damping [38]. As cracks can be treated as dissipative elements which are responsible for the damping process in future studies one should focus on the comparison of a mathematical model with damping and nonlinear rotational springs with the one from this study. The obtained results will show that the increase in the complexity of the mathematical model translates into great differences in the results.

REFERENCES

[1] M.E. Atay and S.B. Coskunb, "Elastic stability of Euler columns with a continuous elastic restraint using variational iteration method," *Comput. Math. Appl.*, vol. 58, no. 11–12, pp. 2528–2534, 2009, doi: 10.1016/j.camwa.2009.03.051.

[2] C.M. Wang, C.Y. Wang, and J.N. Reddy, *Exact solutions for buckling of structural members*, CRC Press LLC, Florida, USA, 2005.

[3] A. Williams, "Elastic instability", in *Structural Analysis in theory and practice*, Elsevier, 2009, pp. 71–99, doi: 10.1016/B978-1-85617-550-0.00004-X.

[4] W. Sochacki, S. Garus, and J. Garus, "Influence of material defects on the dynamic stability of the bernoulli-euler beam," *Arch. Metall. Mater.*, vol. 66, no. 2, pp. 519–522, 2021, doi: 10.24425/amm.2021.135887.

[5] M. Beck, "Die knicklast des einseitig eingespannten, tangential gedrückten Stabes," *J. Appl. Math. Phys.-ZAMP*, vol. 3, pp. 225–228, 1952, doi: 10.1007/BF02008828.

[6] A. Gajewski, "Vibration and stability of a non-prismatic column compressed by non-conservative forces in non-linear creep conditions," *J. Sound Vibr.*, vol. 248, no. 2, pp. 315–327, 2001

[7] G. Herrmann and R.W. Bungay, "One the stability of elastic systems subjected to non-conservative forces", *J. Appl. Mech.*, vol. 31, pp. 435–440, 1964.

[8] J.B. Ryu, Y. Sugiyama, K.B. Yim, and G.S. Lee, "Dynamic stability of an elastically restrained column subjected to triangulary distributed subtangential forces," *Comput. Struct.,* vol.76. pp. 611–619, 2000.

[9] K. Sato, "Instability of a clamped-elastically restrained Timoshenko column carrying a tip load subjected to a follower force," *J. Sound Vibr.*, vol. 194, no. 4, pp. 623–630, 1996.

[10] T.E. Smith and G. Herrman, "Stability of a beam on an elastic foundation subjected to a follower force," *J. Appl. Mech.*, vol. 39, pp. 628–629, 1972

[11] Y. Sugiyama, K. Katayama, and K. Kiriyama, "Experimental verification of dynamic stability of vertical cantilevered columns subjected to a sub-tangential force," *J. Sound Vibr.*, vol. 236, no. 2, pp. 193–207, 2000

[12] H. Leipholz, "Aspects of dynamic stability of structures," *J. Eng. Mech. Div.*, vol. 4, pp. 109–124, 1975.

[13] A.N. Kounadis, "Divergence and flutter instability of elastically restrained structures under follower forces," *Int. J. Eng. Sci.*, vol. 19, no. 4, pp. 553–562, 1981.

[14] J. Przybylski, "The role of prestressing in establishing regions of instability for a compound column under conservative or nonconservative load," *J. Sound Vibr.*, vol. 231, no. 2, pp. 291–305, 2000.

[15] A.N. Kounadis, "The existence of regions of divergence instability for nonconservative systems under follower forces," *Int. J. Solids Struct.*, vol. 19, no. 8, pp. 725–733, 1983.

[16] A. Di Egidio, A. Luongo, and A. Paolone, "Linear and nonlinear interactions between static and dynamic bifurcations of damped planar beams," *Int. J. Non-Linear Mech.*, vol. 42, pp. 88–98, 2007.

[17] A.N. Kounadis, "Stability of elastically restrained Timoshenko cantilevers with attached masses subjected to a follower force," *J. Appl. Mach.*, vol. 44, pp. 731–736, 1977.

[18] A. Flax, "Divergence of cantilever columns under combined conservative and follower loads," *J. Appl. Mech.-Trans. ASME*, vol. 51, no. 2, pp. 187–198, 1984.

[19] L. Tomski and J. Szmidla, "Vibration and stability of column subjected to generalized load by a force directed towards a pole," *J. Theor. Appl. Mech.*, vol. 42, no. 1, pp. 163–193, 2004.

[20] L. Tomski and S. Uzny, "The new realization of the specific load – free vibrations of a column," in *Dynamical Systems, Analytical/Numerical Methods, Stability, Bifurcation and Chaos*, Łódź, Wydawnictwo Politechniki Łódzkiej, 2011, pp. 301–306.

[21] L. Tomski, M. Gołębiowska-Rozanow, and J. Szmidla, "Free vibration of a column loaded by a force and bending moment," *Vibr. Phys. Syst.*, vol. 16, pp. 317–319, 1980.

[22] P. Obara and W. Gilewski, "Dynamic stability of moderately thick beams and frames with the use of harmonic balance and perturbation methods, "*Bull. Pol. Acad. Sci. Tech. Sci.*, vol. 64, no. 4, pp. 739–750, 2016.

[23] L. Mazurkiewicz, D. Kolodziejczyk, K. Damaziak, J. Malachowski, M. Klasztorny, and P. Baranowski, "Load carrying capacity numerical study of I-beam pillar structure with blast protective panel," *Bull. Pol. Acad. Sci. Tech. Sci.*, vol. 61, no. 2, pp. 451–457, 2013.

[24] T.G. Chondros and T.G. Dimarogonas, "Dynamic sensivity of structures to cracks," *J. Vib. Acoust. Stress Reliab. Des.*, vol. 111, pp. 251–256, 1989.

[25] T.G. Chondros, "The continuous crack flexibility model for crack identification," *Fatigue Fract. Eng. Mater. Struct.*, vol. 24, pp. 643–650, 2001.

[26] T.G. Chondros, T.G. Dimarogonas, and J. Yao, "A continuous cracked beam vibration theory," *J. Sound Vibr.*, vol. 215, pp. 17–34, 1998

[27] B. Binici, "Vibration of beams with multiple open cracks subjected to axial forcem," *J. Sound Vibr.*, vol. 287, pp. 277–295, 2005.

[28] J. Lee and L.A. Bergman, "The vibration of stepped beams and rectangular plates by an elemental dynamic flexibility method," *J. Sound Vibr.*, vol. 171, pp. 617–640, 1994.

[29] N. Anifantis and A. Dimarogonas, "Stability of columns with a single crack subjected to follower and axial loads," *Int. J. Solids Struct.*, vol. 19, pp. 281–291, 1981.

[30] G.L. Qian, S.N. Gu., and J.S. Jiang, "The dynamic behavior and crack detection of a beam with a crack," *J. Sound Vibr.*, vol. 225, no. 1, pp. 201–208, 1990.

[31] M. Kucewicz, P. Baranowski, and J. Małachowski, "Dolomite fracture modeling using the Johnson-Holmquist concrete material model: Parameter determination and validation," *J. Rock Mech. Geotech. Eng.*, vol. 13, no. 2, pp. 335–350, 2021.

[32] L. Tomski and S. Uzny, "Vibrations and stability of a column subjected to the specific load realized by circular elements of heads," *Mech. Mech. Eng.*, vol. 17, pp.197–206, 2013.

[33] L. Tomski *et. al*., "Drgania swobodne i stateczność układów smukłych poddanych obciążeniu konserwatywnemu i nie konserwatywnemu," Warszawa, WNT, 2012. (in Polish)

[34] K. Sokół, "An influence of the parameters of the loading heads on stability and free vibrations of a damaged column subjected to a specific load," *J. Vibroeng.*, vol. 20, no. 3, pp. 1299–1310, 2018.

[35] K. Sokół, "The control of stability of a column subjected to specific load," *J. Appl. Math. Comput. Mech.*, vol. 18, no. 4, pp. 8594, 2019

[36] K. Sokół and S. Uzny, "Stability of a damaged slender structure loaded by a force directed towards a positive pole," in *Engineering Mechanics 2016*, 2016, pp. 514–517.

[37] S. Uzny, K. Sokół, and M. Osadnik, "Influence of amplitude on free vibration frequency of a partially tensioned column," in *Engineering Mechanics 2016*, 2016, pp. 562–565

[38] J. Przybylski, "Drgania i stateczność dwuczłonowych układów prętowuych wstępnie sprężonych przy obciążeniach niezachowawczych," Częstochowa, Wydawnicwto PCz, 2002.